Transcriptome analysis of thyroid tissue in patients with Hashimoto's disease using next-generation sequencing: case–control study

Marija Čikotić[1], Marieta Bujak[2], Silvija Piškorjanac[3], Mario Štefanić[4]

[1]University Hospital Centre Zagreb, Zagreb, Croatia

[2]University of Split School of Medicine, Split, Croatia

[3]Faculty of Dental Medicine and Health, Josip Juraj Strossmayer University, Osijek, Croatia

[4]Department of Nuclear Medicine and Oncology, Osijek Faculty of Medicine, Josip Juraj Strossmayer University, Osijek, Croatia

Correspondence to:
Mario Štefanić
Department of Nuclear Medicine and Oncology, Osijek Faculty of Medicine, Josip Juraj Strossmayer University, Josipa Huttlera 4, 31000 Osijek, Croatia
mstefanic@mefos.hr

Cite as:
Čikotić M, Bujak M, Piškorjanac S, Štefanić M. Transcriptome analysis of thyroid tissue in patients with Hashimoto's disease using next-generation sequencing: case–control study. ST-OPEN. 2025;6:e2025.2219.27.

DOI:
https://doi.org/10.48188/so.6.9

Aim: Hashimoto's thyroiditis (HT) is a common but poorly understood autoimmune disease. Here, we aimed to identify differentially expressed genes and biological signaling pathways associated with HT by comparing whole genome transcriptomes from affected and healthy donors.

Methods: As part of a case–control design, we analyzed thyroid tissue RNA sequencing libraries from the Genotype-Tissue Expression Project (v8 release). Donors were divided into two demographically and technically matched groups according to the presence (n = 31) or absence of histopathologically confirmed HT in their thyroid tissue samples (n = 73). Differential gene expression analysis was performed, followed by pathway enrichment profiling (Hallmark, Kyoto Encyclopedia of Genes and Genomes).

Results: In total, we identified 2,809 upregulated genes and 2,348 downregulated genes (fold change >1.5, Benjamini-Hochberg adjusted $P < 0.05$). HT was characterized by pathways associated with T- and B-cell signaling, antigen processing, cytokine-cytokine receptor interactions, phagocytic responses, and cell death. The transition to HT was accompanied by a decreased expression of gene sets related to cell junctions, cell polarity, epithelial and anabolic processes, redox homeostasis, mitochondrial health, and Hippo signaling. Loss of endothelial cell characteristics and positional markers of perivascular fibroblasts followed closely thereafter.

Conclusions: The local expansion of cellular, humoral and innate immunity is a hallmark of HT. Cell death dominated the scene, followed by signs of epithelial, endothelial and stromal remodeling of thyroid tissue. This included reciprocal contraction of the terminally differentiated epithelium and (perivascular) endothelium amidst increasing autoimmune activity. Widespread changes in gene activity were observed in various homeostatic processes, including cell metabolism, cellular energetics, and anabolic and catabolic metabolic pathways.

Keywords: autoimmune; computational biology; gene expression profiling; RNA-seq; thyroiditis; whole genome sequencing

Introduction

Hashimoto's thyroiditis (HT) is a common autoimmune disease characterized by the gradual replacement of thyroid follicular architecture by scar tissue and lymphoplasmocytic aggregates (*1*, *2*). It occurs predominantly in middle-aged women and shows a strong familial segregation, as well as a highly variable course of disease. In most patients, thyroid hormone levels are well maintained in the initial phase; over time, life-threatening primary hypothyroidism often develops (*1*, *2*). The etiology of HT remains poorly understood (*3*), and there are currently very few treatment options beyond lifelong hormone replacement therapy (*4*), which is often insufficient to restore well-being and overall quality of life (*5*–*7*). Thyroid autoimmunity is also associated with pregnancy complications affecting both mother and child (*8*, *9*) and, more importantly, with an increased risk of developing thyroid malignancies (*10*, *11*). There is therefore an urgent need to improve our understanding of the biology of HT.

To achieve this, HT research has recently turned to more advanced technologies, such as next-generation sequencing of bulk tissues and single-cell RNA sequencing (RNA-seq). Both methods allow comprehensive profiling of gene expression on a genome-wide scale and offer a unique opportunity to gain insights into changes in cellular composition and gene activity of complex tissues (*12*, *13*). Consequently, RNA-seq has radically changed our understanding of inflammatory diseases (*12*, *14*), but its application in HT remains modest (*15*–*17*). To date, the highest resolution has been achieved in immune cell lines infiltrating the thyroid gland (*15*–*17*). In contrast, the epithelial and mesenchymal niches have been comparatively understudied (*16*–*18*), due to the low cellular recovery of follicular and stromal components in the single-cell protocols currently in use. In addition, RNA-seq is highly sensitive to technical and biological confounding factors (*19*–*22*), sample size and computational details (*23*), making interpretation of the data an extremely complex task (*15*). Therefore, it remains difficult to draw a comprehensive picture of HT based on the information from these studies alone, and the simultaneous remodeling of the epithelium, immune system and stroma has yet to be replicated in a single study (*17*).

Here, we used publicly available whole genome RNA-seq libraries of thyroid tissue from the Genotype-Tissue Expression (GTEx) project (*24*, *25*) to systematically compare the gene expression profiles of affected individuals with those of healthy donors. Our aim was to better characterize the cascade of transcriptional events and to investigate the extent of thyroid tissue remodeling in HT. To this end, we performed an unbiased screening of deeply phenotyped and carefully annotated datasets (*26*), supported by the extensive literature on best practices in GTEx data (*19*–*22*, *24*–*26*).

Methods

Participants

A total of 104 tissue donors were included in this case–control study. Donors were divided into two independent groups based on the presence or absence of histopathologically confirmed HT in their thyroid tissue samples. The whole-genome gene expression profiles of the thyroid tissue were then integrated, harmonized and compared between the two groups to search for differentially expressed genes and associated biological pathways.

Materials

The study material consisted of whole-genome thyroid tissue libraries (expression matrices, dbGaP phs000424.v8.p2) and associated metadata. The following attributes were recorded for each donor: pathology reports, agonal characteristics, technical characteristics, sample processing characteristics and the first five principal components of the genotype (PC1-5). The PC1-5 components provide information about the structure of the donor population in whole-genome genotyping (*25*). Digitized microscopic images of hematoxylin and eosin-stained thyroid tissue sections from HT patients (Aperio, Leica Biosystems) were downloaded from the GTEx portal. The photomicrographs were visualized using QuPath v0.2.0-m9 (https://github.com/qupath, University of Edinburgh, UK). Anonymous and de-identified RNA-seq data were obtained from the GTEx Project Repository (v8, https://gtexportal.org/home/datasets). The study was approved by the Ethics Committee of the Faculty of Medicine in Osijek (REG. NO. 2158-61-46-22-89; April 30, 2022).

Of the 574 libraries classified as thyroid tissue (UBERON0002046), 184 control samples and 37 thyroid samples showing histopathologic features of HT were selected for further analysis. Degraded samples, mislabeled libraries, neoplasms, thyroid tissue samples with non-specific changes, and contaminated samples with large vessels, thymus, muscle, adipose tissue, and parathyroid tissue were excluded from the selection (*22*, *26*). After adjusting for confounding factors (age, sex, agonal classification on the Hardy scale (*27*), RNA integrity, collection facility, and ischemia time), the final comparison included 73 normal and 31 affected tissue libraries. All libraries were independent (one library per unrelated donor), and all donors were over 21 years of age, with a postmortem interval of less than 24 hours.

RNA sequencing

In brief, RNA sequencing was performed using the Illumina TruSeq protocol (non-stranded, polyA+ selection; Broad Institute; HiSeq 2000 or HiSeq 2500) on 200 ng of total RNA extracted from 0.5–2 g of thyroid tissue (PAXgene Tissue miRNA Kit, PreAnalytix, Qiagen). The target coverage was ~50 million 76-bp reads (*24*, *25*).

RNA read quality, alignment, and quantification

The RNA quality after fixation (PAXgene Tissue FIX, Qiagen) was assessed using the RNA Integrity Number (RIN; Agilent Bioanalyzer), with an exclusion threshold of RIN < 5.5 (*24*, *25*). Alignment to the human reference genome (GRCh38/hg38) was performed using STAR v2.5.3a with GENCODE v26 annotations (56,200 genes). Gene-level quantification was performed by collapsing all gene isoforms into a single transcript.

Gene expression analysis

Expression values were normalized to the effective library size using the Trimmed Mean of M-values (TMM) approach (*28*) from the edgeR package (*29*). Variance stabilization was performed using a rank-based inverse normal transformation (*30*). Systematic variation (*31*) was corrected by applying the function *removeBatchEffect* (first three genotype PCs + hidden factors). Hidden factors (representing batch effects) were identified by nonparametric modeling of the expression matrix using the DASC package (convex clustering and nonnegative matrix factorization, regularization parameter lambda = 10^{-3}-10^{-1}, factorization rank = 2-10, optimal rank according to cophenetic coefficient = 3, L2 penalty, 100 initializations) (*32*).

Transcriptome comparison between HT patients and healthy controls

We tested for differential expression using linear modeling with Bayesian modulation in the limma package (*33*–*35*). Compared to other methods, the *lmFit* function is particularly robust for small samples. We defined differential expression as an absolute fold change (|FC|) greater than 1.5 and corrected for a false discovery rate (FDR) less than 0.05 using the Benjamini-Hochberg procedure.

Biological pathway analysis

Biological pathway analysis (Hallmark and C2 sets (*36*) from the MSigDB v7.4 collection (*37*)) was performed using a list of differentially expressed genes as input. The significance threshold was set to FDR < 0.05 (1,000 permutations) for gene sets with at least 10 genes (*38*). Visualization of the C2 pathway (Kyoto Encyclopedia of Genes and Genomes) was performed using the Pathview package under the GNU General Public License (≥ 3.0) (*39*). The lists of differentially expressed genes were also matched with a table of cell markers (Azimuth 2023) (*40*) and tissue-related transcripts (Human Gene Atlas) from Enrichr (https://maayanlab.cloud/Enrichr/) (*41*). The list of stem cell-associated signatures was obtained from StemChecker (http://stemchecker.sysbiolab.eu/) (*42*).

Gene symbol conversion was performed using the biomaRt package (HUGO Gene Nomenclature Committee/HGNC – Ensembl/ENSG, *H. sapiens*). Gene and transcript classification was based on the Ensembl r105 release. HGNC symbols were used for gene naming throughout the text. The list of matrisome components was retrieved from the M5889 set (the MSigDB collection, Naba_matrisome).

Statistical analysis

Continuous data (demographic and technical attributes) were summarized using the median and interquartile range. Categorical data are presented as absolute frequencies and proportions. Contingency tables were analyzed using Fisher's exact test. For non-genomic continuous variables, the Mann-Whitney test was used to examine the difference between the two independent samples. The nonparametric correlation analysis was based on Spearman's rank test. All *P*-values were two-sided, with *post-hoc* correction for the number of tests described above. Unless otherwise stated, adjusted *P*-values are reported throughout the text. The Multivariate and Propensity Score Matching Software for Causal Inference was used to adjust for confounding factors (*43*). Results were visualized using the packages ComplexHeatMap v2.6.2, RColorBrewer v1.1-2, EnhancedVolcano v1.12.0 and ggpubr v0.4.0 in R, version 4.0.3 (R Foundation for Statistical Computing, Vienna, Austria).

Results

The final analysis included a total of 21,077 genes with unique HGNC symbols. **Table 1** shows the demographic characteristics of the donors and technical details of the samples. The clear separation between affected and control participants indicates a global differ-

Table 1. Donor demographics with sample processing details (n = 104)*

Attributes	Category/unit	HT (n = 31)	Controls (n = 73)	*P*†
Sex	Male/female	12/19	32/41	0.670
Age (years)	20-29	1	2	0.865‡
	30-39	2	8	
	40-49	9	17	
	50-59	6	19	
	60-69	13	27	
Autolysis score (SMATSSCR)	0 (no autolysis)	5	3	0.182
	1 (mild)	22	59	
	2 (moderate)	4	11	
TISCH (SMTSISCH)	min.	452 (121-951)	449 (163-706)	0.924
PAX (SMTSPAX)	min.	824 (653-1089)	776 (631-1077)	0.582
RIN (SMRIN)	-	6.9 (6.4-7.3)	6.7 (6.2-7.2)	0.935
Center (SMCENTER)	B1	23	52	0.815‡
	C1	8	21	
Agonal category (DTHHRDY)	0 (ventilator case)	19	45	0.762‡
	1 (fast death, violent)	1	1	
	2 (fast death, natural)	9	17	
	3 (intermediate, ill)	1	3	
	4 (slow death)	1	7	
Total mapped reads (SMMPPD)	× 10^7	7.66 (6.39-9.24)	7.83 (6.95-8.99)	0.541

*TISCH – ischemic (*post-mortem*) interval, PAX – time spent in PAX fixative, RIN – RNA integrity number, Center – sampling institution. The labels in parentheses are the original abbreviations for specific attributes. Continuous variables are presented as medians with interquartile ranges.
†Mann-Whitney test.
‡Generalized Fisher exact test (Freeman-Halton extension).

ence in gene expression between diseased and healthy thyroid tissue (**Figure 1**). Most of those affected were women over the age of 40, although age and gender were similarly distributed in the control group. The lowest RIN score was 5.5 and the highest recorded score was 9.7. Ten donors had histologically severe/diffuse HT, nine had focal areas of lymphocytic thyroiditis, and the remainder were classified as moderate HT (Figure S1 in our online dataset (*44*)). Broadly speaking, late-stage HT was associated with higher transcriptional variability, but none of these subgroups were large enough to support subgroup analysis. There were no significant differences between groups in terms of sample preservation, ischemia time, tissue fixation, or cause of death. Sequencing depth was similar in both groups.

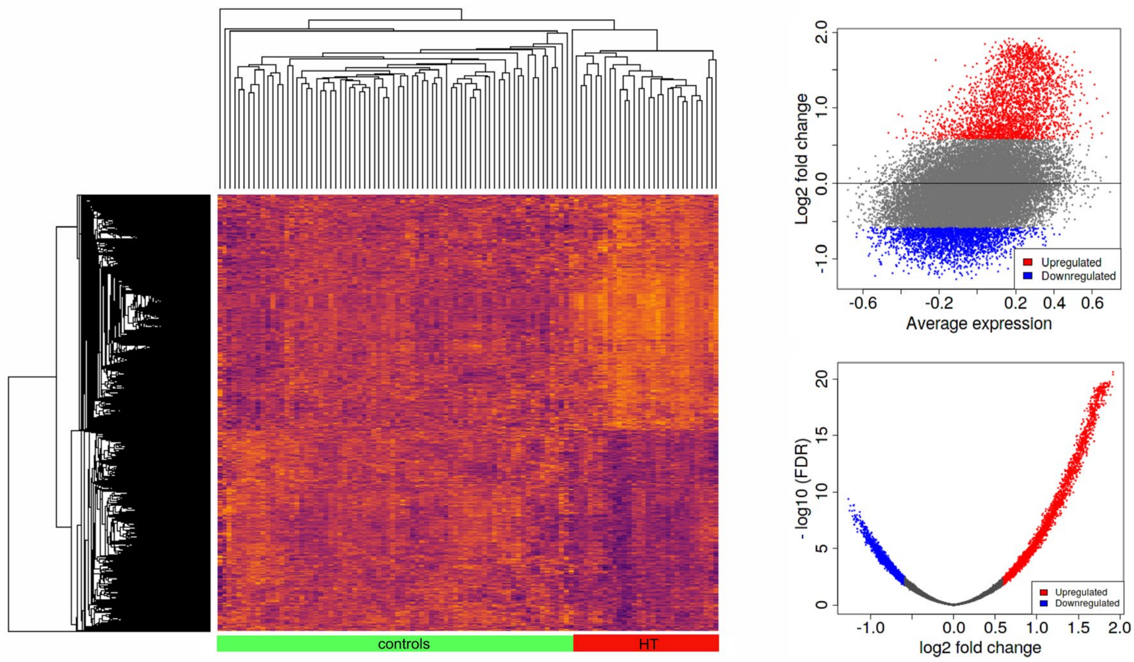

Figure 1. Overview of differentially expressed genes. **Panel A.** Hierarchical clustering (Euclidean distance, method = complete linkage). Lighter shades correspond to higher expression levels. **Panel B.** Bland-Altman representation of differentially expressed genes. FDR – false discovery rate (Benjamini-Hochberg), HT – Hashimoto's thyroiditis. Created using ComplexHeatmap R package (https://www.rdocumentation.org/packages/ComplexHeatmap/versions/1.10.2).

Among differentially expressed transcripts (FDR < 0.05, |FC| > 1.5), 2,809 genes showed significantly higher and 2,348 significantly lower expression in the affected thyroid tissues (**Figure 1**), with the top 45 hits from both lists presented in Table S1 in our online dataset (*44*). Protein-coding genes were the most abundant transcript type, followed by long non-coding RNAs and immunoglobulin variable regions, as presented in Table S2 in our online dataset (*44*). The results of the biological pathway analysis for the C2 and H sets from MSigDB are summarized in **Table 2** and **Table 3**, respectively. Pathway analysis revealed that activation of the immune system was paramount (T cell and B cell signaling, **Figure 2**, along with cell death and cytotoxicity-related processes (**Figure 3**, **Table 2**).

Table 2. Pathway analysis, MSigDB v7.4, Kyoto Encyclopedia of Genes and Genomes*

Process	Enriched			Process	Depleted		
	NES	No. genes	*P**		NES	No. genes	*P*†
Cytokine-cytokine receptor interactions	2.65	227	1.8×10^{-4}	Oxidative phosphorylation	-2.60	110	3.6×10^{-4}
Natural killer cell-mediated cytotoxicity	2.57	87	1.8×10^{-4}	AMPK signaling pathway	-2.12	111	3.6×10^{-4}
Th1 and Th2 cell differentiation	2.44	72	1.8×10^{-4}	Autophagy	-1.96	133	3.7×10^{-4}
T cell receptor signaling	2.41	95	1.8×10^{-4}	Hippo signaling pathway	-1.90	27	4.8×10^{-3}
Th1 cell differentiation	2.37	84	1.8×10^{-4}	Adherent junctions	-1.85	68	1.2×10^{-3}
B cell receptor signaling	2.37	66	1.8×10^{-4}	Insulin signaling pathway	-1.80	128	3.7×10^{-4}
Chemokine signaling	2.36	169	1.8×10^{-4}	Mitophagy	-1.80	65	2.9×10^{-3}
NF-kappa B signaling pathway	2.23	96	1.8×10^{-4}	Selenocompound metabolism	-1.79	15	1.6×10^{-2}
Cell adhesion molecules	2.20	118	1.8×10^{-4}	Tight junctions	-1.77	150	3.9×10^{-4}
Processing and presentation	1.97	36	8.6×10^{-4}	Pentose phosphate pathway	-1.74	24	2.1×10^{-2}
Autoimmune thyroid disease	1.96	16	1.7×10^{-3}	mTOR signaling pathway	-1.69	143	9.7×10^{-4}
Complement and coagulation cascades	1.88	67	5.6×10^{-4}	Glutathione metabolism	-1.68	44	1.6×10^{-2}
Necroptosis	1.86	121	3.6×10^{-4}	Fatty acid metabolism	-1.61	52	2.3×10^{-2}
Leukocyte transendothelial migration	1.80	103	5.9×10^{-4}	Focal adhesions	-1.55	193	3.2×10^{-3}
Apoptosis	1.80	128	4.6×10^{-4}	Axon guidance	-1.54	170	3.0×10^{-3}
Fc receptor-mediated phagocytosis	1.76	86	2.5×10^{-3}				
TNF signaling pathway	1.66	103	5.1×10^{-3}				
Cell cycle	1.51	119	2.2×10^{-2}				

*Abbreviations: Th – T helper, NES – normalized enrichment score, mTOR – mammalian target of rapamycin, AMPK 5’ – adenosine monophosphate-dependent protein kinase, NF – nuclear factor, TNF – tumor necrosis factor.
†Corrected *P*-value.

Table 3. Pathway analysis, MSigDB v7.4, Hallmark*

Process	Enriched expression			Process	Depleted expression		
	NES	No. genes	*P*†		NES	No. genes	*P*†
Allograft rejection	3.12	175	6.9×10^{-5}	Oxidative phosphorylation	-2.69	198	1.7×10^{-4}
Interferon-gamma response	2.90	185	6.9×10^{-5}	Protein secretion	-2.65	95	1.6×10^{-4}
Interferon-alpha response	2.56	89	6.9×10^{-5}	Adipogenesis	-2.38	196	1.7×10^{-4}
IL6 JAK STAT3 signaling	2.47	83	6.9×10^{-5}	Fatty acid metabolism	-2.11	151	1.7×10^{-4}
Inflammatory response	2.45	189	6.9×10^{-5}	Reactive oxygen species	-1.81	45	3.4×10^{-3}
Complement	2.09	187	6.9×10^{-5}	Myogenesis	-1.74	188	1.7×10^{-4}

Table 3. (continued)

Process	Enriched expression NES	No. genes	*P*†	Process	Depleted expression NES	No. genes	*P*†
IL2 STAT5 signaling	2.03	96	6.9×10^{-5}	Androgen response	-1.46	98	2.4×10^{-2}
TNFA signaling via NFKB	2.03	190	6.9×10^{-5}	Xenobiotic metabolism	-1.37	179	1.9×10^{-2}
E2F targets	2.02	197	6.9×10^{-5}	Glycolysis	-1.35	190	2.0×10^{-2}
G2-M checkpoint	1.8	197	6.9×10^{-5}	Epithelial-mesenchymal transition	-1.34	199	2.1×10^{-2}
KRAS signaling up	1.7	188	1.6×10^{-4}				
P53 pathway	1.39	197	3.3×10^{-2}				

*Abbreviations: NES – normalized enrichment score, IL – interleukin, JAK – Janus kinase, STAT – signal transducer and activator of transcription, TNF – tumor necrosis factor.
†Corrected *P*-value.

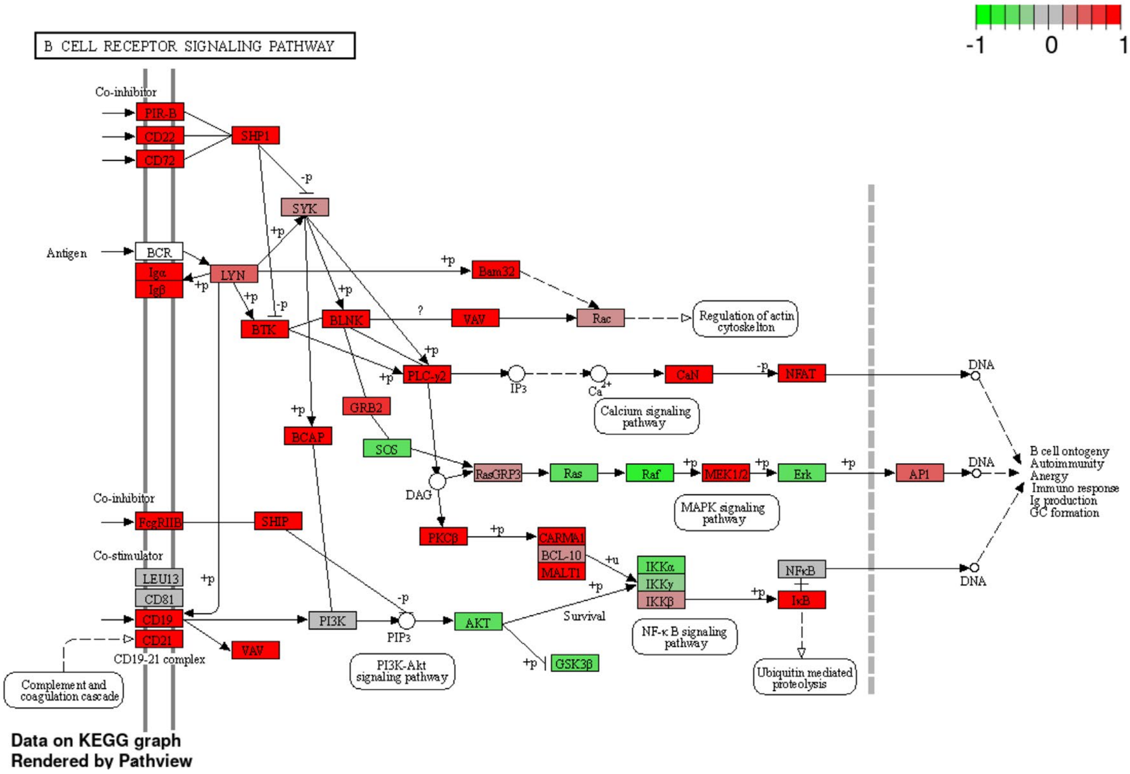

Figure 2. The expression of genes related to the B cell receptor and the distal signaling pathways in the thyroid gland. The figure was generated using the Pathview package under the GNU General Public License (≥ 3.0), based on data from the Kyoto Encyclopedia of Genes and Genomes (KEGG). Gene symbols and their respective names are available at https://www.genenames.org/.

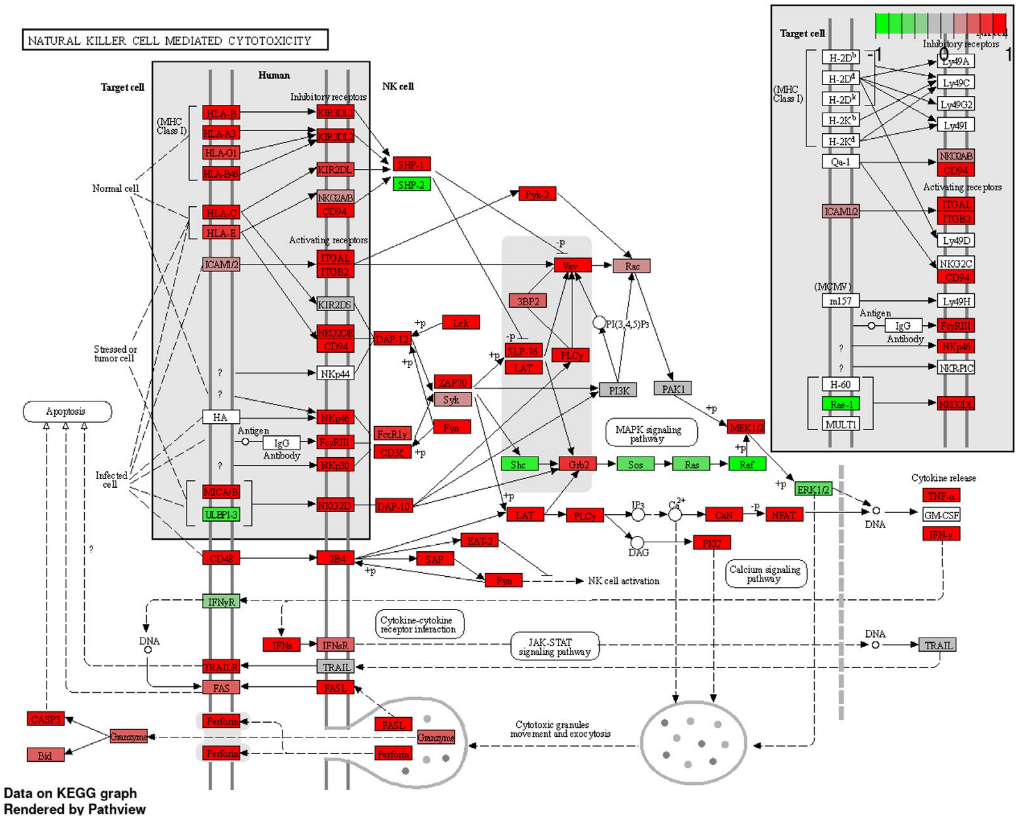

Figure 3. Normalized gene expression of cytotoxic-natural killer cell markers. The figure was generated using the Pathview package under the GNU General Public License (≥ 3.0), based on data from the Kyoto Encyclopedia of Genes and Genomes (KEGG). Gene symbols and their respective names are available at https://www.genenames.org/.

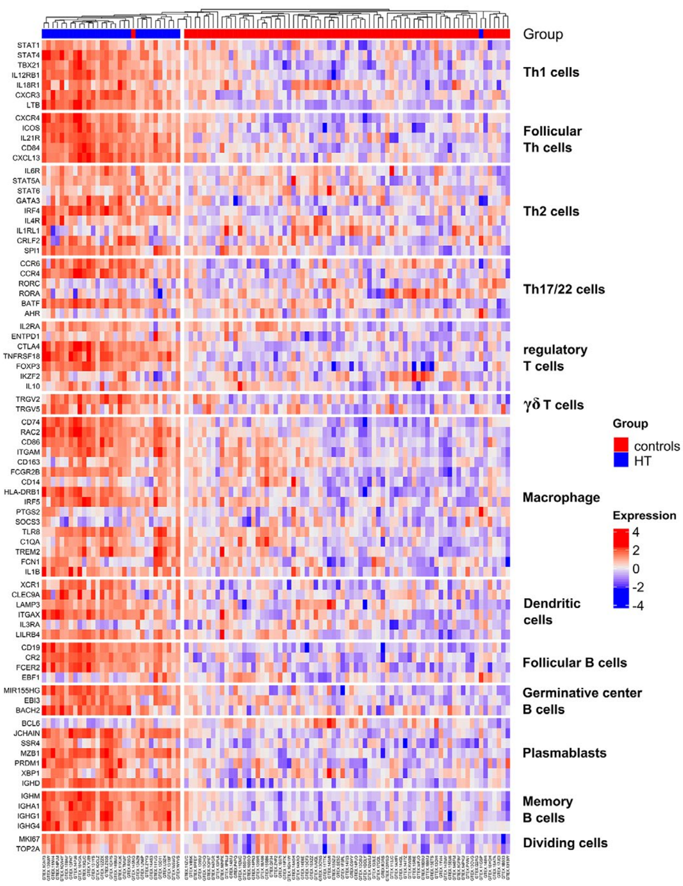

Figure 4. Gene expressions of immune cell lineage markers (z-scale) in thyroid tissues. HT – Hashimoto's thyroiditis. Column names (bottom row) correspond to the original sample identification codes (n = 104). Created using ComplexHeatmap R package (https://www.rdocumentation.org/packages/ComplexHeatmap/versions/1.10.2).

In addition to the T-cell receptor (TCR) chains of conventional (TRAV1−2^{neg}) αβ-T cells, the expression of gamma-chain TCRs (TRGV2/5/7/9-10, TRGC1) was significantly increased. Among the lineage-specific markers (**Figure 4**), the master regulators of T-helper (Th) type 1 and 2 responses were highly enriched. In the B cell lineage (MS4A1, CD79A), the telltale markers of activation and maturation were particularly present (cells of the light and dark zone of the germinal center, plasmablasts, activated and memory B cells). In addition to lymphoid immunity, myeloid markers were also enriched, indicating the presence of macrophages and dendritic cells (FDCSP, $\log_2$FC = 1.21, $P = 2 \times 10^{-9}$, **Figure 4**) (*45*).

Among the highly enriched cytokine gene transcripts, as presented in Figure S2 in our online dataset (*44*), chemotaxis, adhesion and migration were prominent in functional analysis, followed by transendothelial recruitment, lymphoid organization (CCL19, $\log_2$FC = 1.22, $P = 4.3 \times 10^{-9}$; CXCL9, $\log_2$FC = 1.39, $P = 3.9 \times 10^{-12}$) and tissue retention of inflammatory cells (*16*).

Among the downregulated gene transcripts, loss of key components that support cellular architecture and tissue maintenance was evident, along with loss of genes for planar cell polarity (PCP4, FAT4, CELSR2, RYK, PHACTR4; $-0.7 < \log_2$FC < -0.6, $0.0018 < P < 0.0066$) and in-

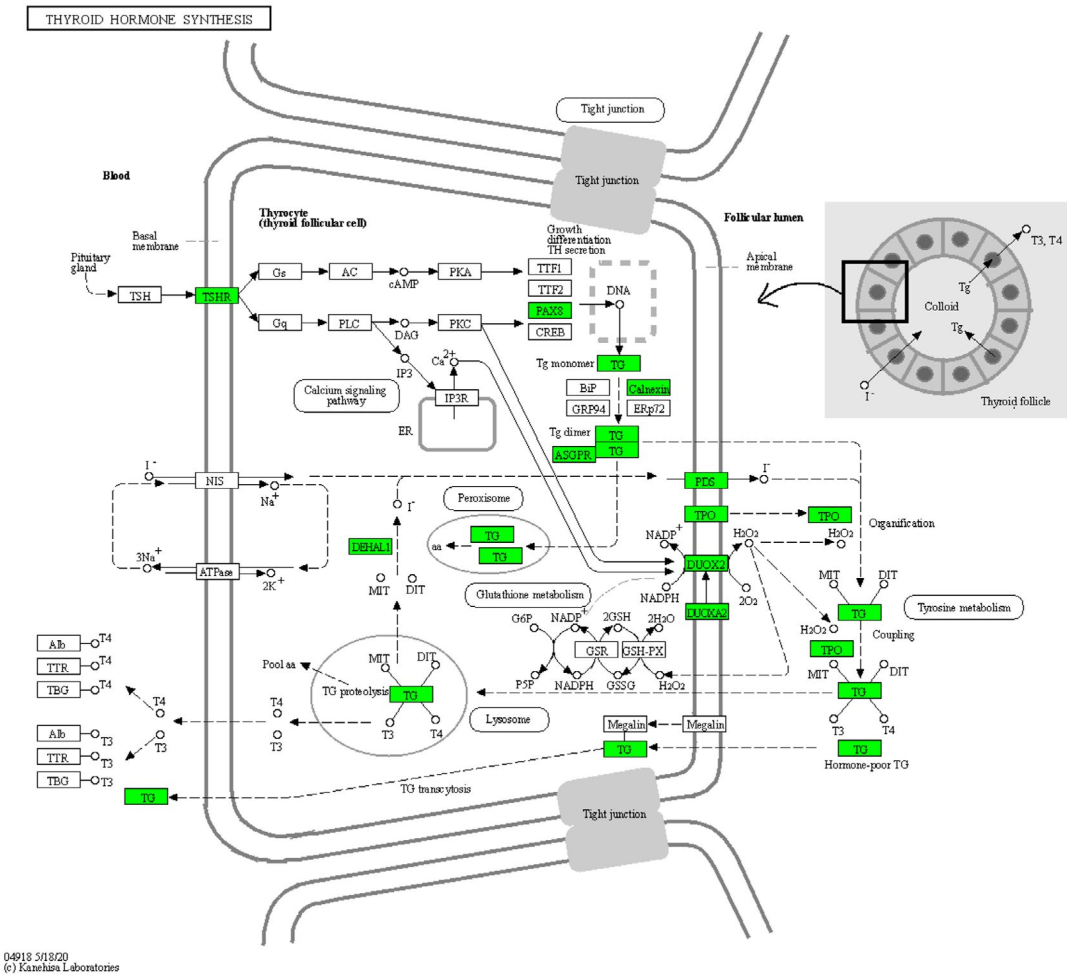

Figure 5. Gene expression from the iodine organification and thyroxine biosynthesis pathways in thyroid tissue. Green color indicates significantly reduced expression (FDR < 0.05). The figure was generated using the Pathview package under the GNU General Public License (≥ 3.0), based on data from the Kyoto Encyclopedia of Genes and Genomes. Gene names are available at https://www.genenames.org/ (HGNC symbols).

tercellular communication (**Table 2**) (*46*). Overall, a significant reduction in thyroid-related characteristics was observed ($P = 5.8 \times 10^{-40}$, Human Gene Atlas).

Epithelial markers were significantly overrepresented among the downregulated transcripts, reflecting a systematic deviation in the expression of transcriptional regulators (NKX2-1, PAX8) and canonical markers of terminally differentiated thyroid follicular cells (DIO1, TSHR, TG, TFF3; Table S1, (*44*)). In addition, there was a pronounced loss of iodine transport and thyroxine biosynthesis (TPO, DUOXA2, IYD/DEHAL1, TG, SLC26A7, SLC26A4/PDS) (**Figure 5**). Besides thyroid epithelial markers a clear loss of endothelial features was observed (CDH5, TIE1, PTPRB, EDNRB, PLVAP, PDPN, PROX1; Table S3, (*44*)), along with reduced angiogenic signaling (VEGFA-FLT1/VEGFC-FLT4), loss of perivascular fibroblastic positional markers (NOTCH3, SPARC, CD36, STEAP4; Figure S1 and Table S3) (*44*, *47*, *48*), and decreased expression of COL4A1 ($\log_2 FC = -0.69$, $P = 2.8 \times 10^{-3}$) and COL18A1 ($\log_2 FC = -0.6$, $P = 5.8 \times 10^{-3}$), two collagens that underlay the epithelial and endothelial cell sheets. The loss of homeostatic basement membrane collagens was mirrored by over-transcription of the genes for type VII (COL7A1, $\log_2 FC = 0.83$, $P = 1.7 \times 10^{-4}$) and type XXII (fibril-associated) collagen (COL22A1, $\log_2 FC = 0.73$, $P = 9.6 \times 10^{-4}$).

The mechanisms of follicular and endothelial cell death are still largely unknown. Possible mechanisms include complement-mediated lysis, which usually depends on antibodies (**Figure 6**, **Table 2**, **Table 3**) and apoptosis as an expression of cellular cytotoxicity (**Table 2**).

Beyond these pathways, transcripts encoding components involved in cellular necroptosis have also been identified, suggesting that there may be an additional level of complexity under specific circumstances, as presented in **Table 2** and Figure S3 (*44*). In addition, there

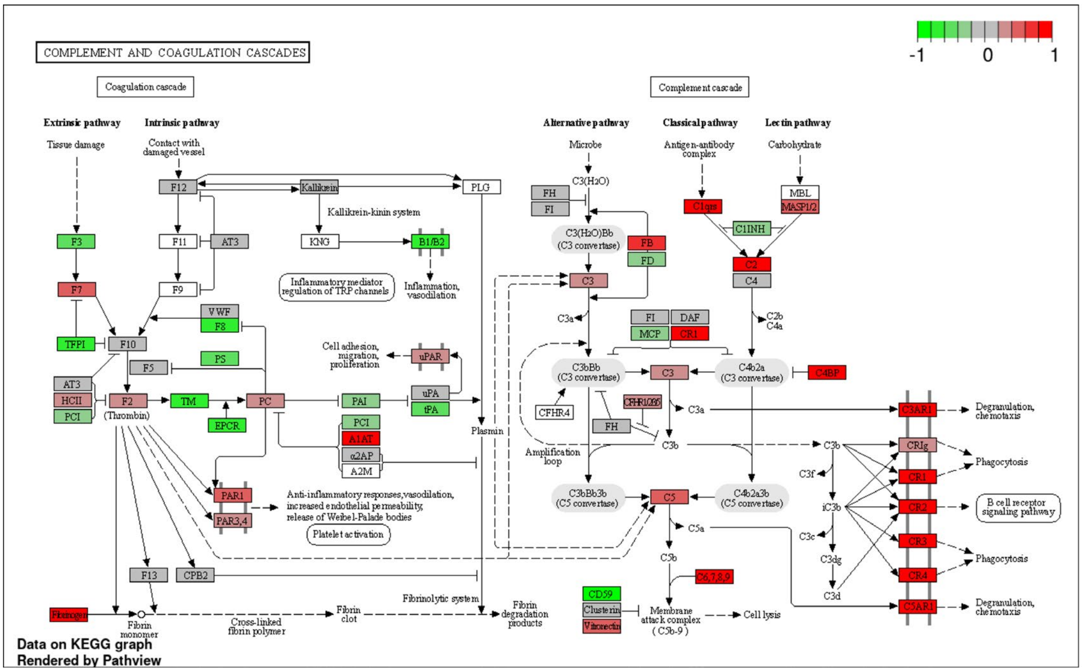

Figure 6. Normalized gene expression, the coagulation pathway (a) and complement pathway (b) in diseased thyroid tissue. The figure was generated using the Pathview package under the GNU General Public License (≥ 3.0), based on data from the Kyoto Encyclopedia of Genes and Genomes. Gene names are available at https://www.genenames.org/ (HGNC symbols).

was disruption of glutathione metabolism (**Table 2**) and loss of oxidative stress-responsive detoxification (**Table 3**), both of which play a central, cytoprotective role in maintaining thyroid follicular cell redox homeostasis. Metabolically, downregulation of anabolic processes (mTOR signaling, insulin signaling, pentose phosphate pathway) coincided with transcriptional dysregulation of autophagy (**Table 2**), mitochondrial dysfunction, impaired oxidative phosphorylation (**Figure 7**, **Table 2**, **Table 3**), and altered lipid catabolism (β-oxidation) (*15*). Apparently, many transcripts associated with stem cell biology were also lost (Table S4, (*44*)), including β-catenin (CTNNB1), a canonical signal transducer from the Wingless signaling pathway ($\log_2$FC = -0.64, $P = 2.9 \times 10^{-3}$), the Wingless co-receptor LRP6 ($\log_2$FC = -1.18, $P = 1.7 \times 10^{-8}$) and Leucine-Rich Repeat-Containing G protein-Coupled Receptor 5, a Wingless target (LGR5, $\log_2$FC = -0.89, $P = 5.9 \times 10^{-5}$). In contrast, a pronounced increase in downstream signaling was observed along the TNFα and interferon-α/γ pathways (**Table 3**).

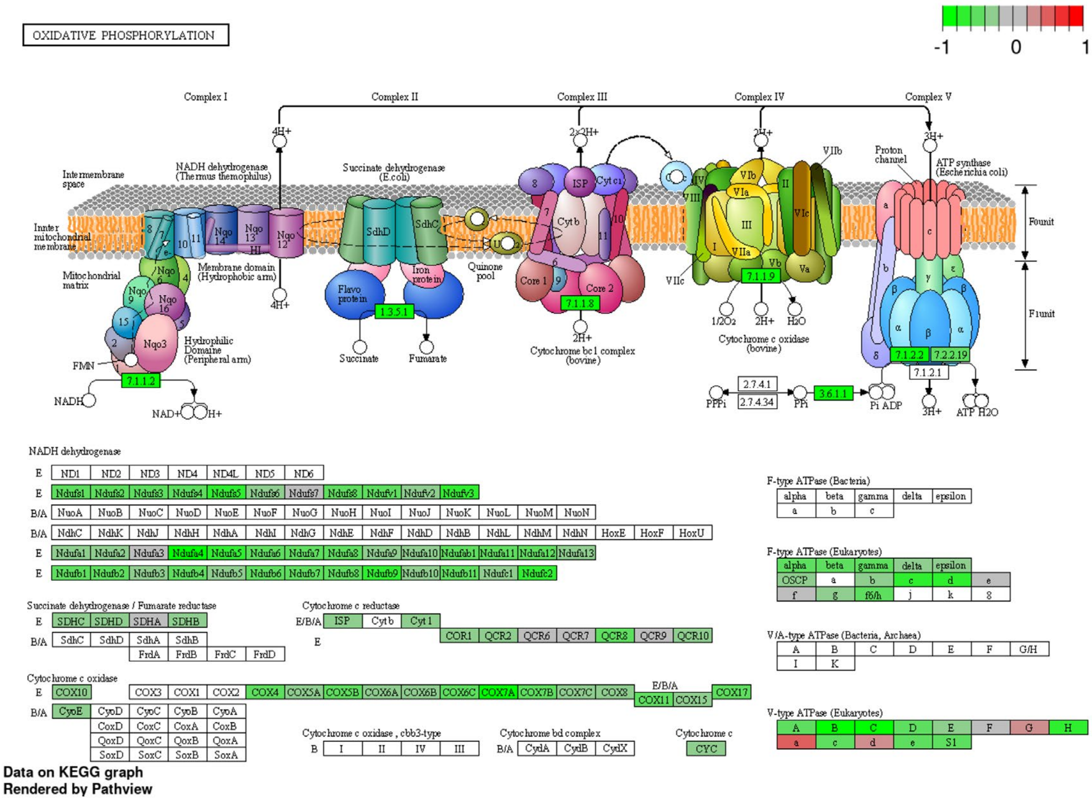

Figure 7. Mitochondrial electron transport chain (oxidative phosphorylation), normalized gene expression in diseased thyroid tissue. The figure was generated using the Pathview package under the GNU General Public License (≥ 3.0), based on data from the Kyoto Encyclopedia of Genes and Genomes. Gene names are available at https://www.genenames.org/.

In addition to the cell-intrinsic transcriptional reprogramming, there were also signs of extensive remodeling of the extracellular matrix, as visible in Figure S4 (*44*). The loss of expression of epithelial markers was accompanied by a strong induction of important fibrogenic factors, such as the transforming growth factor TGFB1 ($\log_2$FC = 0.96, $P = 4.4 \times 10^{-6}$; EPCAM *vs.* TGFB1, Spearman's ρ = -0.3, nominal $P = 0.002$). The increased expression of lysosomal cathepsins (CTS), lysyl oxidases and members of the metalloproteinase superfamily (MMP, ADAM, and ADAMTS proteases) indicates an active remodeling of the cellular microenvironment, as shown in Figure S4 (*44*). Of the 214 differentially expressed genes belonging to extracellular matrix components, 139 were overexpressed.

Discussion

In this study, high-quality whole-genome transcriptomes were used to compare gene expression in healthy and diseased thyroid tissue. The samples reviewed contained detailed donor data, allowing advanced corrections to reduce bias. Documented GTEx procedures ensure reproducible, systematic RNA-seq analysis and provide structured approaches for end users (*26*).

The comparison shows that extensive transcriptional remodeling occurs in thyroid tissue affected by HT, encompassing multiple cell lineages. No cellular niche was spared, with epithelial and endothelial compartments shrinking under the autoimmune assault. Particularly striking is the marked increase in transcripts associated with adaptive immunity and lymphoid organogenesis (T cells, B cells, plasma cells) (*16*, *17*, *49*–*51*), accompanied by increased innate phagocytic activity (*52*, *53*). Both Th1 and Th2 T cell programs have been observed, from transcriptional regulators to cytokines (*3*, *54*, *55*), alongside non-canonical γδ T cells (*56*), whose role remains unclear (*57*). There was also evidence of inflammatory cell recruitment, antigen presentation (*58*, *59*), complement activation, antibody-dependent cytotoxicity, perforin/granzyme-mediated cytolysis and pro-apoptotic signaling (*3*, *60*), consistent with and extending previous findings (*3*, *61*–*63*). These results emphasize that GTEx and bulk RNA-seq are valuable resources when used carefully and provide a unified framework linking previous studies of candidate genes, genetic associations, and animal disease models (*54*).

This study expands the catalog of downregulated transcripts and highlights the loss of signature markers for mature follicular epithelial cells (*17*, *18*, *64*, *65*), decreased expression of molecules critical for epithelial communication, and disruption of the thyroxine biosynthetic pathway (*66*). These findings are consistent with histologic evidence of epithelial destruction and loss of follicular architecture (*1*, *3*), but have often remained elusive in recent mapping efforts (*15*, *16*). We also found transcriptional evidence of mitochondrial (*15*) and ciliary remodeling (*67*–*69*), impaired oxidative phosphorylation, impaired anabolic metabolic pathways, and altered planar cell polarity (*69*, *70*). These results complement the data on the defects in proteostasis (*15*, *71*, *72*) and autophagy (*73*) and provide further details on the functional impairments (*18*). However, the underlying cellular phenotypes remain unclear, as thyroid follicular cells likely exist in transitional states along the epithelial-mesenchymal continuum (*17*, *18*, *64*, *65*, *74*). The effects of HT on epithelial cell composition remain unexplored.

The loss of epithelial markers was accompanied by evidence of endothelial cell dysfunction, with significant but uneven downregulation of canonical endothelial (*75*) and pericyte markers, suggesting (peri)vascular remodeling of the angiofollicular unit (*76*, *77*). These findings are broadly consistent with concepts of stromal and endothelial reprogramming in malignancy and inflammation (*48*, *78*, *79*). In such context, perivascular populations may also act as precursors of specialized fibroblasts (*16*–*18*, *80*), but the fate of the endothelial compartment in HT and its role in thyroid repair or fibrosis remains unclear.

Extensive transcriptional remodeling of the extracellular matrix was observed, including the loss of basement membrane collagens and their replacement by newly produced elements (*81*). Altered expression of enzymes that regulate collagen deposition, cross-linking and matrix turnover was a striking feature of HT thyroids (*17*). Numerous soluble molecules and growth factors with known roles in stromal and epithelial homeostasis, wound healing and stem cell biology were identified (*46*, *77*, *79*, *82*, *83*), linking epithelial-stromal interactions (*16*–*18*) to differentiation of epithelial stem cells in specialized niches (*84*, *85*). The extent of gene deregulation associated with stromal remodeling is consistent with thyroid fibrosis, a hallmark of HT, but provides a deeper understanding of the follicular microenvironment. A complete single cell count of thyroid fibroblasts remains an unmet need.

This transcription atlas provides valuable biomarkers but has important limitations. The results have not been replicated in independent cohorts and no immunohistochemical validation of the markers has been performed, which is important because mRNA levels do not always correlate with protein expression or cell phenotypes. RNA-seq cannot resolve cell-specific gene expression and requires single-cell RNA-seq or scATAC-seq, especially to detect rare cell populations. Combining RNA-seq samples across different histologic stages of HT can highlight large effects while masking subtle changes. Most of the donors were older women, limiting broader applicability. Some of them probably received L-thyroxine (T4), which may affect the expression of inflammatory genes to a small extent (*86*), although it has no effect on overall disease progression.

This study improves and extends the current knowledge of the extent of gene deregulation in thyroid tissue affected by HT. The result of this work is a transcriptomic atlas that improves our understanding of the biology of HT and provides a basis for future translational research.

Provenance: The article is based on the master thesis "Transcriptome analysis of thyroid tissue in patients with Hashimoto's disease by next-generation sequencing" by Marija Čikotić, mag. med. lab. diag., at the Josip Juraj Strossmayer University of Osijek, Faculty of Medicine Osijek under the supervision of Assoc. Prof. Mario Štefanić, PhD, and is deposited in the repository of Faculty of Medicine (https://repozitorij.mefos.hr/islandora/object/mefos%3A1630).

Received: 4 December 2024 / **Accepted:** 24 July 2025 / **Published online:** 17 October 2025

Peer review: Externally peer reviewed.

Acknowledgements: The results published here are in part based upon data generated by the Genotype-Tissue Expression (GTEx) Project (https://commonfund.nih.gov/gtex). The GTEx Project is supported by the Common Fund of the Office of the Director of the NIH, and by National Cancer Institute, National Human Genome Research Institute, National Heart, Lung, and Blood Institute, National Institute on Drug Abuse, National Institute of Mental Health, and National Institute of Neurological Disorders and Stroke. Date of access: 20 Oct 2019.

Ethics considerations: The study was approved by the Ethics Committee of the University of Osijek Faculty of Medicine (Reg. No. 2158-61-46-22-89).

Funding: No funding was received for this study.

Authorship declaration: All authors conceptualized the article, participated in the writing, revising, editing, and finalizing the manuscript. All authors read and approved the final manuscript and they all take accountability for the work.

Availability of data: Supplementary figures and tables for this study are available at the Open Science Framework: https://osf.io/639s2/?view_only=209ef4e6159645369a6d935fcd18531f (*44*).

Disclosure of interest: The authors completed the ICMJE Disclosure of Interest Form and disclosed no relevant interests.

ORCID

Marieta Bujak https://orcid.org/0000-0001-9926-3203

Silvija Piškorjanac https://orcid.org/0009-0002-6133-4285

Mario Štefanić https://orcid.org/0000-0001-8995-6137

References

1. Pearce EN, Farwell AP, Braverman LE. Thyroiditis. N Engl J Med. 2003 Jun 26;348(26):2646–55. doi: 10.1056/NEJMra021194
2. Ragusa F, Fallahi P, Elia G, Gonnella D, Paparo SR, Giusti C, et al. Hashimotos' thyroiditis: epidemiology, pathogenesis, clinic and therapy. Best Pract Res Clin Endocrinol Metab. 2019 Dec;33(6):101367. doi: 10.1016/j.beem.2019.101367
3. Stassi G, De Maria R. Autoimmune thyroid disease: new models of cell death in autoimmunity. Nat Rev Immunol. 2002 Mar;2(3):195–204. doi: 10.1038/nri750
4. Wiersinga WM. Paradigm shifts in thyroid hormone replacement therapies for hypothyroidism. Nat Rev Endocrinol. 2014 Mar;10(3):164–74. doi: 10.1038/nrendo.2013.258
5. Hegedüs L, Bianco AC, Jonklaas J, Pearce SH, Weetman AP, Perros P. Primary hypothyroidism and quality of life. Nat Rev Endocrinol. 2022 Apr;18(4):230–42. doi: 10.1038/s41574-021-00625-8
6. Feller M, Snel M, Moutzouri E, Bauer DC, de Montmollin M, Aujesky D, et al. Association of thyroid hormone therapy with quality of life and thyroid-related symptoms in patients with subclinical hypothyroidism: A systematic review and meta-analysis. JAMA. 2018 Oct 2;320(13):1349–59. doi: 10.1001/jama.2018.13770
7. Lillevang-Johansen M, Abrahamsen B, Jørgensen HL, Brix TH, Hegedüs L. Over- and under-treatment of hypothyroidism is associated with excess mortality: a register-based cohort study. Thyroid. 2018 May;28(5):566–74. doi: 10.1089/thy.2017.0517
8. Carafone L, Knutson AJ, Gigliotti BJ. A review of autoimmune thyroid diseases and their complex interplay with female fertility. Semin Reprod Med. 2024 Sep;42(3):178–92. doi: 10.1055/s-0044-1795160
9. De Leo S, Pearce EN. Autoimmune thyroid disease during pregnancy. Lancet Diabetes Endocrinol. 2018 Jul;6(7):575–86. doi: 10.1016/S2213-8587(17)30402-3
10. McLeod DSA, Watters KF, Carpenter AD, Ladenson PW, Cooper DS, Ding EL. Thyrotropin and thyroid cancer diagnosis: a systematic review and dose–response meta-analysis. J Clin Endocrinol Metab. 2012 Aug;97(8):2682–92. doi: 10.1210/jc.2012-1083
11. Resende de Paiva C, Grønhøj C, Feldt-Rasmussen U, von Buchwald C. Association between Hashimoto's thyroiditis and thyroid cancer in 64,628 patients. Front Oncol. 2017 Apr 10;7:53. doi: 10.3389/fonc.2017.00053
12. Stark R, Grzelak M, Hadfield J. RNA sequencing: the teenage years. Nat Rev Genet. 2019 Nov;20(11):631–56. doi: 10.1038/s41576-019-0150-2
13. McCombie WR, McPherson JD, Mardis ER. Next-generation sequencing technologies. Cold Spring Harb Perspect Med. 2019 Nov 1;9(11). doi: 10.1101/cshperspect.a036798

14. Chen H, Ye F, Guo G. Revolutionizing immunology with single-cell RNA sequencing. Cell Mol Immunol. 2019 Mar;16(3):242–9. doi: 10.1038/s41423-019-0214-4

15. Cho BA, Yoo SK, Song YS, Kim SJ, Lee KE, Shong M, et al. Transcriptome network analysis reveals aging-related mitochondrial and proteasomal dysfunction and immune activation in human thyroid. Thyroid. 2018 May;28(5):656–66. doi: 10.1089/thy.2017.0359

16. Zhang QY, Ye XP, Zhou Z, Zhu CF, Li R, Fang Y, et al. Lymphocyte infiltration and thyrocyte destruction are driven by stromal and immune cell components in Hashimoto's thyroiditis. Nat Commun. 2022 Feb 9;13(1):775. doi: 10.1038/s41467-022-28120-2

17. Martínez-Hernández R, Sánchez de la Blanca N, Sacristán-Gómez P, Serrano-Somavilla A, Muñoz De Nova JL, Sánchez Cabo F, et al. Unraveling the molecular architecture of autoimmune thyroid diseases at spatial resolution. Nat Commun. 2024 Jul 13;15:5895. doi: 10.1038/s41467-024-50192-5

18. Massalha H. Trinh MK, Armingol E, Tuck L, Predeus A, Mazin P, et al. A developmental cell atlas of the human thyroid gland. bioRxiv. 2024 Aug 22:2024.08.22.609152. [Preprint]. doi: 10.1101/2024.08.22.609152

19. Leek JT, Scharpf RB, Bravo HC, Simcha D, Langmead B, Johnson WE, et al. Tackling the widespread and critical impact of batch effects in high-throughput data. Nat Rev Genet. 2010 Oct;11(10):733–9. doi: 10.1038/nrg2825

20. Ferreira PG, Muñoz-Aguirre M, Reverter F, Sá Godinho CP, Sousa A, Amadoz A, et al. The effects of death and post-mortem cold ischemia on human tissue transcriptomes. Nat Commun. 2018 Feb 13;9(1):490. doi: 10.1038/s41467-017-02772-x

21. van den Brink SC, Sage F, Vértesy Á, Spanjaard B, Peterson-Maduro J, Baron CS, et al. Single-cell sequencing reveals dissociation-induced gene expression in tissue subpopulations. Nat Methods. 2017 Sep 29;14:935–6. doi: 10.1038/nmeth.4437

22. Nieuwenhuis TO, Yang SY, Verma RX, Pillalamarri V, Arking DE, Rosenberg AZ, et al. Consistent RNA sequencing contamination in GTEx and other data sets. Nat Commun. 2020 Apr 22;11(1):1933. doi: 10.1038/s41467-020-15821-9

23. Luecken MD, Theis FJ. Current best practices in single-cell RNA-seq analysis: a tutorial. Mol Syst Biol. 2019 Jun 19;15(6):e8746. doi: 10.15252/msb.20188746

24. GTEx Consortium. The Genotype-Tissue Expression (GTEx) project. Nat Genet. 2013 Jun;45(6):580–5. doi: 10.1038/ng.2653

25. GTEx Consortium. Human genomics. The Genotype-Tissue Expression (GTEx) pilot analysis: multitissue gene regulation in humans. Science. 2015 May 8;348(6235):648–60. doi: 10.1126/science.1262110

26. Carithers LJ, Ardlie K, Barcus M, Branton PA, Britton A, Buia SA, et al. A novel approach to high-quality postmortem tissue procurement: the GTEx Project. Biopreserv Biobank. 2015 Oct;13(5):311–9. doi: 10.1089/bio.2015.0032

27. Hardy JA, Wester P, Winblad B, Gezelius C, Bring G, Eriksson A. The patients dying after long terminal phase have acidotic brains; implications for biochemical measurements on autopsy tissue. J Neural Transm. 1985;61:253–64. doi: 10.1007/BF01251916

28. Robinson MD, Oshlack A. A scaling normalization method for differential expression analysis of RNA-seq data. Genome Biol. 2010;11(3):R25. doi: 10.1186/gb-2010-11-3-r25

29. Robinson MD, McCarthy DJ, Smyth GK. edgeR: a Bioconductor package for differential expression analysis of digital gene expression data. Bioinformatics. 2010 Jan 1;26(1):139–40. doi: 10.1093/bioinformatics/btp616

30. Chien LC. A rank-based normalization method with the fully adjusted full-stage procedure in genetic association studies. PLoS One. 2020 Jun 19;15(6):e0233847. doi: 10.1371/journal.pone.0233847

31. Leek JT, Johnson WE, Parker HS, Jaffe AE, Storey JD. The sva package for removing batch effects and other unwanted variation in high-throughput experiments. Bioinformatics. 2012 Mar;28(6):882–3. doi: 10.1093/bioinformatics/bts034

32. Yi H, Raman AT, Zhang H, Allen GI, Liu Z. Detecting hidden batch factors through data-adaptive adjustment for biological effects. Bioinformatics. 2018 Apr;34(7):1141–7. doi: 10.1093/bioinformatics/btx630

33. Robinson MD, Smyth GK. Moderated statistical tests for assessing differences in tag abundance. Bioinformatics. 2007 Nov;23(21):2881–7. doi: 10.1093/bioinformatics/btm453

34. Ritchie ME, Phipson B, Wu D, Hu Y, Law CW, Shi W, et al. limma powers differential expression analyses for RNA-sequencing and microarray studies. Nucleic Acids Res. 2015 Apr 20;43(7):e47. doi: 10.1093/nar/gkv007

35. Phipson B, Lee S, Majewski IJ, Alexander WS, Smyth GK. Robust hyperparameter estimation protects against hypervariable genes and improves power to detect differential expression. Ann Appl Stat. 2016 Jun;10(2):946–63. doi: 10.1214/16-AOAS920

36. Kanehisa M, Furumichi M, Tanabe M, Sato Y, Morishima K. KEGG: new perspectives on genomes, pathways, diseases and drugs. Nucleic Acids Res. 2017 Jan 4;45(D1):D353–D361. doi: 10.1093/nar/gkw1092

37. Liberzon A, Birger C, Thorvaldsdóttir H, Ghandi M, Mesirov JP, Tamayo P. The Molecular Signatures Database (MSigDB) hallmark gene set collection. Cell Syst. 2015 Dec 23;1(6):417–25. doi: 10.1016/j.cels.2015.12.004

38. Tilford CA, Siemers NO. Gene set enrichment analysis. In: Nikolsky Y, Bryant J, editors. Protein networks and pathway analysis. Methods in Molecular Biology, vol 563. Totowa, NJ: Humana Press; 2009. p. 99–121. doi: 10.1007/978-1-60761-175-2_6

39. Luo W, Brouwer C. Pathview: an R/Bioconductor package for pathway-based data integration and visualization. Bioinformatics. 2013 Jul;29(14):1830–1. doi: 10.1093/bioinformatics/btt285

40. Hao Y, Hao S, Andersen-Nissen E, Mauck WM 3rd, Zheng S, Butler A, et al. Integrated analysis of multimodal single-cell data. Cell. 2021 Jun 24;184(13):3573–87.e29. doi: 10.1016/j.cell.2021.04.048

41. Xie Z, Bailey A, Kuleshov MV, Clarke DJB, Evangelista JE, Jenkins SL, et al. Gene set knowledge discovery with Enrichr. Curr Protoc. 2021 Mar;1(3):e90. doi: 10.1002/cpz1.90

42. Pinto JP, Kalathur RK, Oliveira DV, Barata T, Machado RS, Machado S, et al. StemChecker: a web-based tool to discover and explore stemness signatures in gene sets. Nucleic Acids Res. 2015 Jul 1;43(W1):W72–7. doi: 10.1093/nar/gkv529

43. Sekhon JS. Multivariate and propensity score matching software with automated balance optimization: the matching package for R. J Stat Soft. 2011 Jun 14;42(7):1–52. doi: 10.18637/jss.v042.i07

44. Bujak M. Transcriptome analysis of thyroid tissue in patients with Hashimoto's disease using next-generation sequencing [Internet]. 2025. [cited 2025 Sep 5]. Available from https://osf.io/639s2/?view_only=209ef4e6159645369a6d935fcd18531f

45. Domínguez Conde C, Xu C, Jarvis LB, Rainbow DB, Wells SB, Gomes T, et al. Cross-tissue immune cell analysis reveals tissue-specific features in humans. Science. 2022 May 13;376(6594):eabl5197. doi: 10.1126/science.abl5197

46. Butler MT, Wallingford JB. Planar cell polarity in development and disease. Nat Rev Mol Cell Biol. 2017 Jun;18(6):375–88. doi: 10.1038/nrm.2017.11

47. Winkler EA, Kim CN, Ross JM, Garcia JH, Gil E, Oh I, et al. A single-cell atlas of the normal and malformed human brain vasculature. Science. 2022 Mar 4;375(6584):eabi7377. doi: 10.1126/science.abi7377

48. Korsunsky I, Wei K, Pohin M, Kim EY, Barone F, Major T, et al. Cross-tissue, single-cell stromal atlas identifies shared pathological fibroblast phenotypes in four chronic inflammatory diseases. Med (New York, N.Y.). 2022 Jul 8;3(7):481–518.e14. doi: 10.1016/j.medj.2022.05.002

49. Tang H, Zhu M, Qiao J, Fu YX. Lymphotoxin signalling in tertiary lymphoid structures and immunotherapy. Cell Mol Immunol. 2017;14:809–18. doi: 10.1038/cmi.2017.13

50. Marinkovic T, Garin A, Yokota Y, Fu YX, Ruddle NH, Furtado GC, et al. Interaction of mature CD3+CD4+ T cells with dendritic cells triggers the development of tertiary lymphoid structures in the thyroid. J Clin Invest. 2006 Oct;116(10):2622–32. doi: 10.1172/JCI28993

51. Furtado GC, Marinkovic T, Martin AP, Garin A, Hoch B, Hubner W, et al. Lymphotoxin beta receptor signaling is required for inflammatory lymphangiogenesis in the thyroid. Proc Natl Acad Sci USA. 2007 Mar 20;104(12):5026–31. doi: 10.1073/pnas.0606697104

52. Sanin DE, Ge Y, Marinkovic E, Kabat AM, Castoldi A, Caputa G, et al. A common framework of monocyte-derived macrophage activation. Sci Immunol. 2022 Apr 15;7(70):eabl7482. doi: 10.1126/sciimmunol.abl7482

53. Villani AC, Satija R, Reynolds G, Sarkizova S, Shekhar K, Fletcher J, et al. Single-cell RNA-seq reveals new types of human blood dendritic cells, monocytes, and progenitors. Science. 2017 Apr 21;356(6335):eaah4573. doi: 10.1126/science.aah4573

54. Yang X, Gao T, Shi R, Zhou X, Qu J, Xu J, et al. Effect of iodine excess on Th1, Th2, Th17, and Treg cell subpopulations in the thyroid of NOD.H-2h4 mice. Biol Trace Elem Res. 2014;159:288–96. doi: 10.1007/s12011-014-9958-y

55. Shi Y, Wang H, Su Z, Chen J, Xue Y, Wang S, et al. Differentiation imbalance of Th1/Th17 in peripheral blood mononuclear cells might contribute to pathogenesis of Hashimoto's thyroiditis. Scand J Immunol. 2010;72:250–5. doi: 10.1111/j.1365-3083.2010.02425.x

56. Liu H, Zheng T, Mao Y, Xu C, Wu F, Bu L, et al. γδ T cells enhance B cells for antibody production in Hashimoto's thyroiditis, and retinoic acid induces apoptosis of the γδ T cell. Endocrine. 2016;51:113–22. doi: 10.1007/s12020-015-0631-9

57. Pizzolato G, Kaminski H, Tosolini M, Franchini DM, Pont F, Martins F, et al. Single-cell RNA sequencing unveils the shared and the distinct cytotoxic hallmarks of human TCRVδ1 and TCRVδ2 γδ T lymphocytes. Proc Natl Acad Sci USA. 2019 Jun 11;116(24):11906–15. doi: 10.1073/pnas.1818488116

58. Jacobson EM, Huber A, Tomer Y. The HLA gene complex in thyroid autoimmunity: from epidemiology to etiology. J Autoimmun. 2008 Feb–Mar;30(1–2):58–62. doi: 10.1016/j.jaut.2007.11.010

59. Zeitlin AA, Heward JM, Newby PR, Carr-Smith JD, Franklyn JA, Gough SC, et al. Analysis of HLA class II genes in Hashimoto's thyroiditis reveals differences compared to Graves' disease. Genes Immun. 2008;9:358–63. doi: 10.1038/gene.2008.26

60. Liu Y, You R, Yu N, Gong Y, Qu C, Zhang Y, et al. Increased proportions of Tc17 cells and NK cells may be risk factors for disease progression in Hashimoto's thyroiditis. Int Immunopharmacol. 2016 Nov;40:332–8. doi: 10.1016/j.intimp.2016.09.016

61. Ajjan RA, Weetman AP. The Pathogenesis of Hashimoto's Thyroiditis: Further Developments in our Understanding. Horm Metab Res. 2015;47(10):702–10. doi: 10.1055/s-0035-1548832

62. Liu J, Mao C, Dong L, Kang P, Ding C, Zheng T, et al. Excessive iodine promotes pyroptosis of thyroid follicular epithelial cells in Hashimoto's thyroiditis through the ROS-NF-κB-NLRP3 pathway. Front Endocrinol (Lausanne). 2019 Nov 20;10:778. doi: 10.3389/fendo.2019.00778

63. Hwangbo Y, Park YJ. Genome-Wide Association Studies of Autoimmune Thyroid Diseases, Thyroid Function, and Thyroid Cancer. Endocrinol Metab (Seoul). 2018 Jun;33(2):175–84. doi: 10.3803/EnM.2018.33.2.175

64. Liang J, Qian J, Yang L, Chen X, Wang X, Lin X, et al. Modeling human thyroid development by fetal tissue-derived organoid culture. Adv Sci (Weinh). 2022;9:e2105568. doi: 10.1002/advs.202105568

65. Liao T, Zeng Y, Xu W, Shi X, Shen C, Du Y, et al. A spatially resolved transcriptome landscape during thyroid cancer progression. Cell Rep Med. 2025 Apr 15;6(4):102043. doi: 10.1016/j.xcrm.2025.102043

66. Chaker L, Razvi S, Bensenor IM, Azizi F, Pearce EN, Peeters RP. Hypothyroidism. Nat Rev Dis Primers. 2022;8:30. doi: 10.1038/s41572-022-00357-7

67. Lee J, Yi S, Eun Kang Y, Young Chang J, Tae Kim J, Joung Sul H, et al. Defective ciliogenesis in thyroid Hürthle cell tumors is associated with increased autophagy. Oncotarget. 2016;7(48):79117–30. doi: 10.18632/oncotarget.12997

68. Lee J, Park KC, Sul HJ, Hong HJ, Kim KH, Kero J, et al. Loss of primary cilia promotes mitochondria-dependent apoptosis in thyroid cancer. Sci Rep. 2021 Feb 18;11(1):4181. doi: 10.1038/s41598-021-83418-3

69. Martínez-Hernández R, Serrano-Somavilla A, Ramos-Leví A, Sampedro-Nuñez M, Lens-Pardo A, Muñoz De Nova JL, et al. Integrated miRNA and mRNA expression profiling identifies novel targets and pathological mechanisms in autoimmune thyroid diseases. EBioMedicine. 2019 Dec;50:329–42. doi: 10.1016/j.ebiom.2019.10.061

70. Koumarianou P, Gómez-López G, Santisteban P. Pax8 controls thyroid follicular polarity through cadherin-16. J Cell Sci. 2017 Jan 1;130(1):219–31. doi: 10.1242/jcs.184291

71. Wright MT, Kouba L, Plate L. Thyroglobulin interactome profiling defines altered proteostasis topology associated with thyroid dyshormonogenesis. Mol Cell Proteomics. 2021;20:100008. doi: 10.1074/mcp.RA120.002168

72. Read ML, Brookes K, Thornton CEM, Fletcher A, Nieto HR, Alshahrani M, et al. Targeting non-canonical pathways as a strategy to modulate the sodium iodide symporter. Cell Chem Biol. 2022 Mar 17;29(3):502–12.e7. doi: 10.1016/j.chembiol.2021.07.016

73. Zheng T, Xu C, Mao C, Mou X, Wu F, Wang X, et al. Increased interleukin-23 in Hashimoto's thyroiditis disease induces autophagy suppression and reactive oxygen species accumulation. Front Immunol. 2018 Jan 29;9:96. doi: 10.3389/fimmu.2018.00096

74. Yang RM, Song SY, Wu FY, Yang RF, Shen YT, Tu PH, et al. Myeloid cells interact with a subset of thyrocytes to promote their migration and follicle formation through NF-κB. Nat Commun. 2023 Dec 6;14(1):8082. doi: 10.1038/s41467-023-43895-8

75. Becker LM, Chen SH, Rodor J, de Rooij LPMH, Baker AH, Carmeliet P. Deciphering endothelial heterogeneity in health and disease at single cell resolution: progress and perspectives. Cardiovasc Res. 2023 Mar 17;119(1):6–27. doi: 10.1093/cvr/cvac018

76. Buechler MB, Pradhan RN, Krishnamurty AT, Cox C, Calviello AK, Wang AW, et al. Cross-tissue organization of the fibroblast lineage. Nature. 2021 May;593(7860):575–9. doi: 10.1038/s41586-021-03549-5

77. Muhl L, Genové G, Leptidis S, Liu J, He L, Mocci G, et al. Single-cell analysis uncovers fibroblast heterogeneity and criteria for fibroblast and mural cell identification and discrimination. Nat Commun. 2020 Aug 7;11(1):3953. doi: 10.1038/s41467-020-17740-1

78. Davidson S, Coles M, Thomas T, Kollias G, Ludewig B, Turley S, et al. Fibroblasts as immune regulators in infection, inflammation and cancer. Nat rev Immunol. 2021 Nov;21(11):704–17. doi: 10.1038/s41577-021-00540-z

79. Lendahl U, Muhl L, Betsholtz C. Identification, discrimination and heterogeneity of fibroblasts. Nat Commun. 2022 Jun 14;13(1):3409. doi: 10.1038/s41467-022-30633-9

80. Di Carlo SE, Peduto L. The perivascular origin of pathological fibroblasts. J Clin Invest. 2018 Jan 2;128(1):54–63. doi: 10.1172/JCI93558

81. Bignon M, Pichol-Thievend C, Hardouin J, Malbouyres M, Bréchot N, Nasciutti L, et al. Lysyl oxidase-like protein-2 regulates sprouting angiogenesis and type IV collagen assembly in the endothelial basement membrane. Blood. 2011 Oct 6;118(14):3979–89. doi: 10.1182/blood-2010-10-313296

82. Nakata Y, Mayassi T, Lin H, Ghosh K, Segerstolpe Å, et al. Genetic vulnerability to Crohn's disease reveals a spatially resolved epithelial restitution program. Sci Transl Med. 2023 Oct 25;15(719):eadg5252. doi: 10.1126/scitranslmed.adg5252

83. Trempus CS, Papas BN, Sifre MI, Bortner CD, Scappini E, Tucker CJ, et al. Functional Pdgfra fibroblast heterogeneity in normal and fibrotic mouse lung. JCI INsight. 2023 Nov 22;8(22):e164380. doi: 10.1172/jci.insight.164380

84. Kato K, Diéguez-Hurtado R, Park DY, Hong SP, Kato-Azuma S, Adams S, et al. Pulmonary pericytes regulate lung morphogenesis. Nat Commun. 2018 Jun 22;9(1):2448. doi: 10.1038/s41467-018-04913-2

85. Kim JE, Fei L, Yin WC, Coquenlorge S, Rao-Bhatia A, Zhang H, et al. Single-cell and genetic analyses reveal conserved populations and signaling mechanisms of gastrointestinal stromal niches. Nat Commun. 2020 Jan 17;11(1):334. doi: 10.1038/s41467-019-14058-5

86. Wang L, Li Z, Wan R, Pan X, Li B, Zhao H, et al. Single-cell RNA sequencing provides new insights into therapeutic roles of thyroid hormone in idiopathic pulmonary fibrosis. Am J Respir Cell Mol Biol. 2023 Oct;69(4):456–69. doi: 10.1165/rcmb.2023-0080OC